Institute of Paper Science and Technology
Atlanta, Georgia

IPST Technical Paper Series Number 643

Corrosion of Composite Tube Air Ports in Kraft Recovery Boiler — Cr_2O_3 Solubility in NaOH

M. Estes, A. Rudie, and J. Colwell

February 1997

INSTITUTE OF PAPER SCIENCE AND TECHNOLOGY
PURPOSE AND MISSIONS

The Institute of Paper Science and Technology is a unique organization whose charitable, educational, and scientific purpose evolves from the singular relationship between the Institute and the pulp and paper industry which has existed since 1929. The purpose of the Institute is fulfilled through three missions, which are:

- to provide high quality students with a multidisciplinary graduate educational experience which is of the highest standard of excellence recognized by the national academic community and which enables them to perform to their maximum potential in a society with a technological base; and

- to sustain an international position of leadership in dynamic scientific research which is participated in by both students and faculty and which is focused on areas of significance to the pulp and paper industry; and

- to contribute to the economic and technical well-being of the nation through innovative educational, informational, and technical services.

ACCREDITATION

The Institute of Paper Science and Technology is accredited by the Commission on Colleges of the Southern Association of Colleges and Schools to award the Master of Science and Doctor of Philosophy degrees.

NOTICE AND DISCLAIMER

The Institute of Paper Science and Technology (IPST) has provided a high standard of professional service and has put forth its best efforts within the time and funds available for this project. The information and conclusions are advisory and are intended only for internal use by any company who may receive this report. Each company must decide for itself the best approach to solving any problems it may have and how, or whether, this reported information should be considered in its approach.

IPST does not recommend particular products, procedures, materials, or service. These are included only in the interest of completeness within a laboratory context and budgetary constraint. Actual products, procedures, materials, and services used may differ and are peculiar to the operations of each company.

In no event shall IPST or its employees and agents have any obligation or liability for damages including, but not limited to, consequential damages arising out of or in connection with any company's use of or inability to use the reported information. IPST provides no warranty or guaranty of results.

Corrosion of Composite Tube Air Ports in Kraft Recovery Boiler– Cr_2O_3 Solubility in NaOH

By Matthew Estes, Alan Rudie, and Jeffery Colwell

Abstract

Composite tubes in kraft recovery boiler air ports can experience severe corrosion. One possibility is the corrosion is caused by molten NaOH. The corrosion of stainless steel in molten salts is dependent upon maintaining the protective Cr_2O_3 film formed on the surface. The goal of this project was to measure the solubility of Cr_2O_3 as a function of the basicity of NaOH. Plots of the chromium ion concentration indicate a minimum solubility at $-\log a_{(Na_2O)}$ of 8.2. The data support two mechanisms for dissolution of the Cr_2O_3. The basic dissolution had a slope of -0.988, consistent with the formation of Na_2CrO_4. The acidic dissolution had a slope of 1.48, consistent with the formation of Cr^{3+}. The results from weight loss experiments on chromium metal were then compared to the solubility curves for Cr_2O_3 to confirm that metal oxide solubility was the rate limiting step in the corrosion mechanism. The weight loss experiments on chromium metal also confirmed that the corrosion rate was a function of the basicity of molten NaOH. Understanding the mechanisms and the environment in which minimum solubility occurs for chromium oxide allows a solution to be proposed to lessen the composite tube air port corrosion of kraft recovery boilers.

Introduction

In recent years, the frequency of corrosion in recovery boiler air ports has risen dramatically throughout the pulp and paper industry (1-5). The increase coincides with the growing use of composite tubes, which are fabricated with a stainless steel outer shell and carbon steel inner body. A unique characteristic of air port corrosion is that the stainless steel is rapidly attacked, exposing the carbon steel underneath. Stainless steel corrosion rates up to 150 mils per year (mpy) have been measured (1-5). After completely consuming the stainless steel, corrosion of the underlying carbon steel occurs at a rate of 10 mpy (1-5). However, there is some concern that the carbon steel can suffer sulfidation corrosion, which was the reason for using composite tubes in air ports.

Molten sodium hydroxide has been postulated as a possible cause for corrosion at air ports (1-3, 5). The severity and uniformity of corrosion are consistent with a molten salt reaction. It has been suggested that sodium hydroxide vaporizing from the smelt bed can migrate to the air port (1). The walls of the air port at 275 to 500°C are relatively cool (4-6). At these temperatures, sodium hydroxide vapors would condense on the waterwall tube surface as a liquid.

There is some evidence for NaOH being present at kraft recovery boiler air ports. Colwell and Fonder collected deposit samples on a cooled probe and measured the melting point *in situ* inside a kraft recovery boiler. Analysis of a limited deposit showed a Na:K ratio of approximately 6:1. The melting points measured yielded a value close to the theoretical melting point of NaOH:KOH of 6 to 1 ratio (3).

Laboratory experimentation has shown that molten sodium hydroxide corrodes stainless steel faster than carbon steel (3). Other corrosive mechanisms in addition to molten NaOH may take place as suggested by Falat (6), but they do not explain why stainless steel corrodes faster than carbon steel.

Theory of molten salt reactions

The stability of an oxide layer on a metal is a function of the oxide's thermodynamics, growth kinetics, and the dissolution of that oxide in the environment. Solubility of an oxide can be defined as the maximum weight of metal ions in solution divided by the weight of the solution. Solubility of a nominally protective oxide is often a function of the salt basicity; where solubility is the defining mechanism, the corrosion rate should also be a function of basicity.

Basicity of a molten salt is defined on the basis of the dissociation of the compound, in this case, NaOH:

$$2\,\text{NaOH} = \text{Na}_2\text{O} + \text{H}_2\text{O} \qquad (1)$$
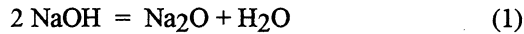
For sodium hydroxide, sodium oxide is defined as the Brönsted base because it accepts a proton, and water is defined as the Brönsted acid because it donates a proton. Basicity, for NaOH, can also be defined by $-\log a_{(\text{Na}_2\text{O})}$, analogous to the definition of pH.

A considerable volume of work has been reported in the literature showing the solubility of different metal ions plotted as function of basicity as shown in Figure 1 (7-15).

Figure 1: Measured oxide solubilities in Na_2SO_4 at 1200°K (12).
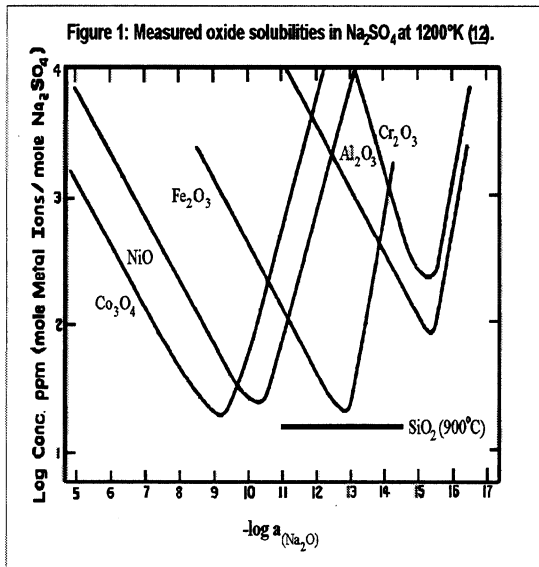
The plots have basicity values along the x-axis and the solubility limit of the metal oxide along the y-axis. These plots show the basicity conditions that give the minimum solubility for a particular metal oxide. If the basicity conditions for a metal oxide is located to the left side of the minimum, the material undergoes a basic dissolution mechanism such as:

$$\text{M}_x\text{O}_Y + \text{O}^{2-} = \text{M}_x\text{O}^{2-}_{Y+1} \qquad (2)$$
where M = metal   O = oxygen
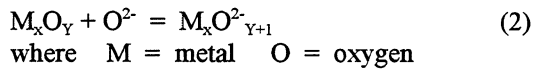
If the basicity conditions for a metal oxide is located to the right side of the minimum, the material undergoes an acidic dissolution mechanism, which is:

$$\text{M}_x\text{O}_Y = X\,\text{M}^{a+} + Y\,\text{O}^{2-} \qquad (3)$$
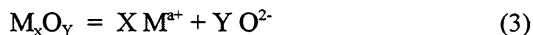
Thus, the location on the curve provides information about which type of dissolution is occurring.

In addition, based on various assumed soluble ions, the dependence of the solubility of a particular ion on basicity can be related to the experimental slope of the curve. An example of acidic dissolution would be:

$$\left(\frac{-\log M^{a+}}{-\log O^{2-}} \right) = \frac{Y}{X} \qquad (4)$$

Agreement between the experimental slopes and theoretical slopes based on stoichiometric equations can be used to confirm the identity of the soluble ion (2).

Equipment

A schematic cross section of the furnace, the crucibles holding the sample, and the electrodes to measure basicity is shown in Figure 2.


Figure 2: Equipment setup
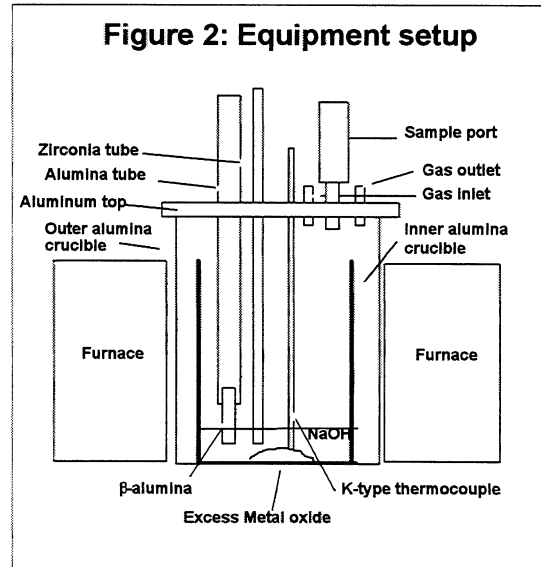
The ceramic crucibles were surrounded by a cylindrical radiant furnace that provided uniform heating. Temperature was measured with a calibrated K-type thermocouple protected by an α-alumina tube and was controlled by a CN3201 Omega® controller. An aluminum top and a silicone O-ring encapsulating in Teflon®, sealed the top of the crucible. Port holes fitted with Cajon® vacuum fittings with Viton® O-rings

provided access to the reactor for the thermocouples, gas inlet and outlets, and electrodes.

Electrodes were inserted into the melt to measure the basicity (16-17). The electrode system consisted of a combination of a β-alumina probe and a zirconia probes. β-alumina ($Al_2O_3 * 5\ Na_2O$) conducts sodium ions exclusively. The ß-alumina tubes were purchased from Polyceram and attached using a Durabond 989™ adhesive to an α-alumina tube to minimize the expense. The inside of the tube was filled with sodium metal, in contact with a platinum wire that was routed outside and sealed. A potential across the ceramic tube wall results from a difference in sodium activity.

Zirconia fully stabilized with yttria ($ZrO_2 * Y_2O_3$) conducts oxygen ions exclusively. The inside end of a closed-end tube was painted with three coats of platinum paste and attached to a platinum wire. The tube was open to the air and thus uses the oxygen in air as a reference. A potential across the ceramic tube wall results from a difference in the oxygen activity.

The half-cell reaction at each electrode is as follows:

Oxidation: $2\ [Na \rightarrow Na^+ + e^-]$ (5)

Reduction: $\frac{1}{2}\ O_2 + 2e^- \rightarrow O^{2-}$ (6)
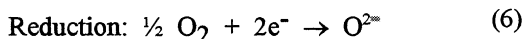
Using the Nerst equation, it follows that

$$E = E° - \frac{RT}{ZF} \ln a_{(i)} \qquad (7)$$

where Z represents the moles of electrons participating in the reaction. For our case with NaOH, equation (7) becomes

$$E = E° - \frac{RT}{2F} \ln a + \frac{RT}{F} \ln (Na) +$$
$$\frac{RT}{4F} \ln P(O_2) \qquad (8)$$

Using pure Na metal as the reference, in the standard state (Na) is unity and ln (Na)=0.

$$E = E° - \frac{RT}{2F} \ln a_{(Na_2O)} + \frac{RT}{4F} \ln P(O_2) \qquad (9)$$

R is equal to $8.314\ J * mol^{-1} * K^{-1}$, and F is equal to 96484.6 C/mol. The temperature, T, was held constant at 773 K for the experiments. Because atmospheric air was the reference for the zirconia tube, the $P(O_2)$ was equal to 0.21 atm. By measuring the voltage, E, the resultant activity of sodium oxide was used to determine the basicity of the sodium hydroxide melt.

The E° value in equation (9) was experimentally determined as follows: first, the sodium hydroxide was completely dried at 500°C under nitrogen gas for three days to remove excess water and contaminants. Then, the basicity was changed by adding sodium oxide to the sodium hydroxide in different concentrations, and the corresponding voltage was measured. A plot of the mole fraction of sodium oxide versus the measured voltage is shown in Figure 3.

Figure 3: Value for E'.

$y = -0.1644x + 0.5669$
$R^2 = 0.9769$
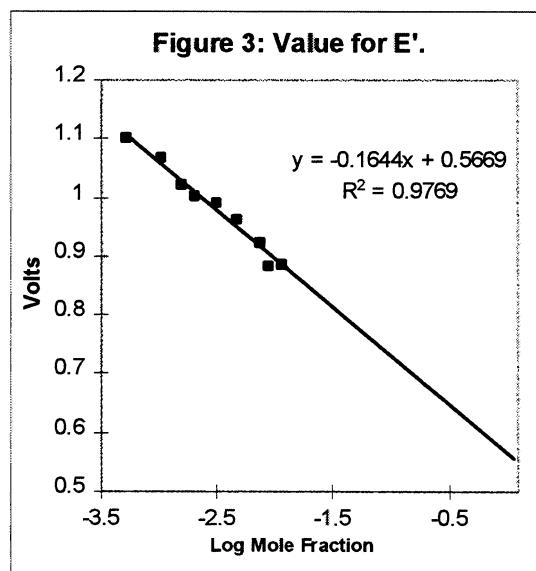
Extrapolating the line to zero sodium oxide content gives E° = 0.567.

For the experiments, sodium oxide was added to make the NaOH more basic. Sodium oxide pellets were purchased from Aldrich®.

To make NaOH more acidic water vapor was added by bubbling the carrier gas through a water column fitted with a polyurethane frit. By fixing the water column temperature and assuming saturation, which was tested by Schwerdtfeger, the vapor pressure was determined (18).

Samples for chemical analysis were collected by inserting a ceramic rod through a ball valve on the aluminum top. The depth of rod insertion was calibrated so that samples of

3

approximately the same size and nearly the same area were obtained. The cold rod caused the sample to freeze to the rod as it was withdrawn from the melt. The sample was then quickly scraped off with ceramic tweezers into a volumetric flask partially filled with deionized water. The weight change of the flask was recorded. The flask was then filled to the mark with deionized water and stored until analyzed. Four replicate salt samples were taken at each basicity.

Chromium concentration was measured using a Perkin Elmer Optima 3000 Dual View Inductively Coupled Plasma (ICP) Spectrometer. Standards were prepared, values loaded into the computer, and then compared with unknown samples using EPA's guidelines for solid waste (19). The optimal conditions for the ICP had been found to be a pressure of 70 psi for argon and wavelength 267 nm for chromium. Chromium gave a linear response from 0.04 ppm to 100 ppm. Each unknown sample was analyzed three times, and the average value was reported.

Results and Discussion

Results for the chromium concentration vs. basicity are summarized in Figure 4 below.

Figure 4: Cr_2O_3 in NaOH.
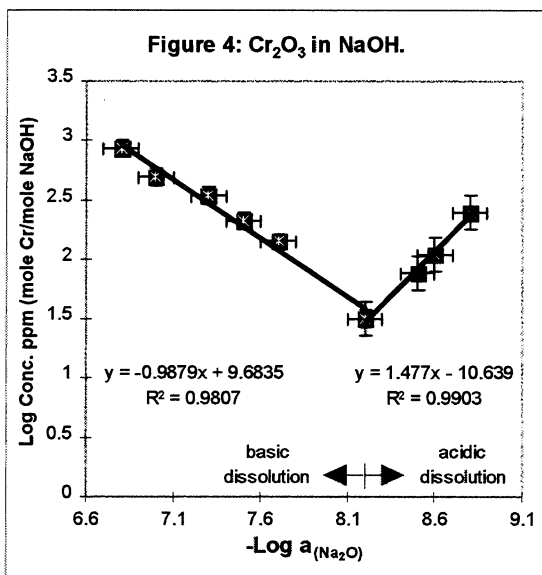
Each basicity condition shown in Figure 4 is a mean of three values. Equilibrium was ensured at a given basicity by measuring until the concentration did not change over three days.

Chromium oxide was found to have a minimum solubility at a basicity of 8.2. The solid line represents the least squares best fit of the data. Basicity error bars were estimated at $-\log a_{(Na_2O)}$ ± 0.1 based upon fluctuations in the voltage readings. Concentration of chromium error bars show ± one standard deviation.

If the dissolution reaction for basic conditions is assumed to be:

$$Cr_2O_3 + 2\ O^{2-} + \frac{3}{2}O_2 = 2\ CrO_4^{2-} \qquad (10)$$
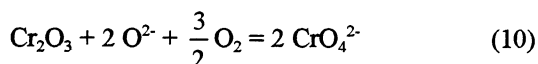
At constant $P(O_2)$,

the theoretical slope for the reaction is given by:

$$\left(\frac{-\log CrO_4^{2-}}{-\log O^{2-}}\right) = -1 \qquad (11)$$

The measured value of -0.9879 is in very good agreement with theory. Also, the melt was yellow in color, which is consistent with the formation of chromate (20).

If the dissolution reaction for acidic conditions is assumed to be:

$$Cr_2O_3 = 2\ Cr^{3+} + 3\ O^{2-} \qquad (12)$$
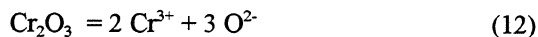
The theoretical slope for the reaction is given by:

$$\left(\frac{-\log Cr^{3+}}{-\log O^{2-}}\right) = \frac{3}{2} \qquad (13)$$

The measured value of 1.477 is in very good agreement with theory. Also, the melt was green in color, which is consistent with the formation of chromium ions (20).

To further confirm that the mechanism for dissolution had changed, the oxidation state of the chromium ion was determined. A chemical method described by Cranston and Murray was used (21). Chromium (III) was scavenged by reacting the solution with 0.01 M iron(III) hydroxide at pH 8. The chromium was precipitated and collected on a 0.45 μm Nucleapore™ filter precleaned with 12 M HCl. The chromium complex was then dissolved in 6 M HCl and analyzed by ICP. Chromium (VI) and chromium(III) are both precipitated by reacting the solution with iron(II) hydroxide at

pH 8. The iron(II) was oxidized to iron(III), and the chromium(VI) was reduced. The precipitated chromium was dissolved in 6 M HCl and analyzed as before. Chromium (VI) was determined by the difference.

Results indicate that the mechanism for dissolution had changed under different basicity conditions on either side of the minimum. Cr(III) was the dominant species at $-\log a_{(Na_2O)}$ of 8.8, and Cr(VI) was the dominant species at $-\log a_{(Na_2O)}$ of 6.8. The change in the oxidation state of chromium confirms that the mechanism changed from basic to acidic dissolution.

Weight loss experiments

Weight loss experiments were performed using chromium metal in molten NaOH at basicity values of 6.8, 8.2, and 8.8. The three basicities selected represented basic dissolution, the solubility minimum, and an acidic dissolution, respectively. Figure 5 shows the results of the weight loss measurements performed at different basicities.

Figure 5: Chromium weight loss in NaOH at 500°C.
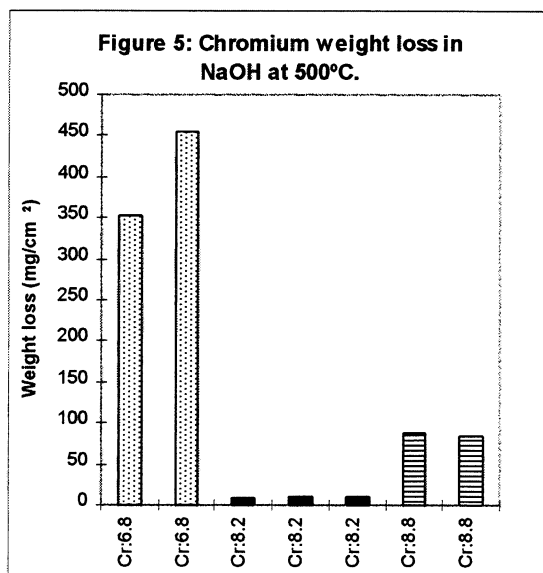
The weight loss variation can be predicted from the basicity and solubility curves. The chromium oxide solubility results in Figure 4 show that the solubility was at a minimum at a basicity value of 8.2. The weight loss of chromium metal is also low at a basicity value of 8.2.

At basicities of 6.8 and 8.8, the solubilities were much higher, which should lead to higher weight loss. Furthermore, the weight

loss at a basicity value of 6.8 should be higher than at 8.8 based upon the solubility curve in Figure 4. Weight loss experiments with chromium metal at basicities of 6.8 and 8.8 in Figure 5 showed the predicted increase in weight loss. Therefore, basicity, which determines the solubility, does affect the weight loss of chromium metal.

In addition, three samples of chromium metal were placed in NaOH at a basicity value of 8.2. The minimum of the chromium oxide solubility was chosen to determine the effect of time on weight loss. After 15 days, the samples were removed and cleaned with water to remove excess NaOH. The samples were then ultrasonically cleaned for 5 minutes in acetone and dried in a desiccator prior to weighing. The same samples were replaced in the furnace with fresh NaOH for an additional 15 days. In figure 6, the results were graphed showing the weight changes of three 15-day trials.

Figure 6: Weight loss as a function of time for Cr in NaOH at a basicity value of 8.2 at 500°C.
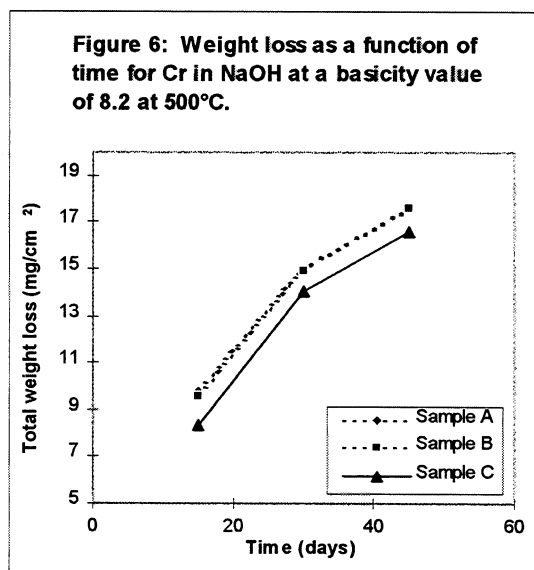
Samples taken from the melt were analyzed by the ICP. The samples were yellow, indicating the presence of chromate, so the basicity was slightly on the basic side of the minimum. The average results are summarized in Table 1.

Table 1: Analysis for chromium by ICP

	Log chromium (ppm)
1st 15 days	2.70
2nd 15 days	1.18
3rd 15 days	0

The results show that the weight loss decreased each time a new trial began. The chromium ions in the melt also identically decreased in each trial until no chromium was detectable.

The kinetic reaction is a first-order reaction. Visually, a dark green, fairly compact scale formed on the test pieces that was strongly adherent to the metal. Because the chromium oxide was minimally soluble in NaOH under the tested conditions, the chromium oxide was able to form a passive layer, which reduced the rate of corrosion. Because the melt was replaced at each 15-day interval, the drop in corrosion rate was not due to the melt becoming saturated.

Conclusion

The solubility of Cr_2O_3 was determined as a function of basicity. The results clearly show a minimum solubility at $-\log a_{(Na_2O)}$ of 8.2. The data suggest two mechanisms of dissolution of chromium oxide in molten NaOH. Basic dissolution (basicity values < 8.2) formed chromate, and acidic dissolution (basicity values > 8.2) formed chromium ions. Analysis of the oxidation state of chromium confirmed the products.

The solubility curves successfully predicted the variation in the weight loss of chromium metal. Chromium coupons at $-\log a_{(Na_2O)}$ of 8.2, which is the minimum solubility of chromium oxide in NaOH, developed a green film that successfully lessened the corrosion.

Controlling conditions in the kraft recovery boiler air ports that establish a minimum solubility condition should lead to a lower corrosion rate of composite tubes. The basicity of a NaOH deposit in a kraft recovery boiler could be controlled by the amount of water vapor in the incoming air to reduce the corrosion rate and provide significant cost savings. The practicality of such an approach would have to be demonstrated. Addition factors, such as the presence of and effect of other metal oxides and chemical species should be investigated further.

Acknowledgments

References

1. Bruno, F. Primary air register corrosion in kraft recovery boilers. Pulp and Paper International Corrosion Problem. 4:68-75. (1983)
2. Colwell, J.A. On the mechanism of corrosion of composite tubes at ports in kraft recovery boilers. 7th International symposium on corrosion, NACE. (1992)
3. Colwell, J.A. and G. Fonder. Status report to the corrosion control project advisory committee. Institute of Paper Science and Technology Unpublished Results. March 24 (1994)
4. Lunn, M.A., W.B.A. Sharp, J.D. Andrews, H.N. Tran, and D. Barham. Corrosion of composite tubes at recovery boiler air ports - A case history. 6th International symposium on corrosion in the pulp and paper industry, NACE. 151-162. (1989)
5. Wensley, D.A. Corrosion of recovery boiler waterwall composite tubes. Corrosion, NACE. (28): 53-55. (1987)
6. Falat, Lad. Corrosion of air ports. Tappi Journal. 79(2): 175-185. (1996)
7. Deanhardt, M.L. and K.H. Stern. Solubility of yttrium oxide in Na_2SO_4 and NaCl melts. Journal of electrochemical society: Electrochemical science and technology. 29(10): 2228-2232. (1982)
8. Gupta, D.K. and R.A. Rapp. The solubilities of NiO, Co_3O_4, and ternary oxides in fused Na_2SO_4 at 1200°K. Journal of electrochemical society: solid-state science and technology. 127(10): 2194-2656. (1980)
9. Hwang, Y.S. and R.A. Rapp. Synergistic dissolution of oxides in molten sodium sulfate. Journal of electrochemical society. 137(4): 1276-1280. (1990)
10. Jose, P.D., D.K. Gupta, and R.A. Rapp. Solubility of α-Al_2O_3 in fused Na_2SO_4 at 1200°K. Journal of electrochemical society. Solid-state science and technology. 132(3): 735-737. (1985)

11. Leblanc, P. and R.A. Rapp. Solubility of Cr_2O_3 in Na_2SO_4-K_2SO_4-$Fe_2(SO_4)_3$. Progress report submitted to E.P.R.I. (11): 1-8. (1991)

12. Leblanc, P. and R.A. Rapp. Solubility of Cr_2O_3 in Na_2SO_4-K_2SO_4-$Fe_2(SO_4)_3$. Behavior of the SO_3 sensor in more reduced environments. Progress report submitted to E.P.R.I. (3): 1-4. (1992)

13. Rapp, R.A. and K.S. Goto. The hot corrosion of metals by molten salts, in molten salts. Ed. J. Braunstein and J.R. Selman. Electrochemical society, Pennington, NH. 81. (1981)

14. Zhang, Y.S. Solubilities of Cr_2O_3 in fused Na_2SO_4 at 1200°K. Journal of electrochemical society: Solid-state science and technology. 133(3): 655-657. (1986)

15. Zhang, Y.S. and R.A. Rapp. Solubility of α-Fe_2O_3 in Fused Na_2SO_4 at 1200°K. Journal of electrochemical society. Solid-state science and technology. 13: 734-735. (1985)

16. Ito, Y. Electrochemical studies on molten sodium hydroxide. Journal of electroanalytical chemistry. 124: 229-235. (1981)

17. Petric, A. Development of cation substituted beta alumina solid electrolytes and EMF measurement of the thermodynamic properties of ionic alloys. Ph.D. Thesis. University of Montreal. (1987)

18. Schwerdtfeger, K. and E.T. Turkdogan. Equilibria and transport phenomena. Physicochemical measurements in metals research. Ed. R.A. Rapp. Interscience Publishers of John Wiley & Sons Inc., New York. 321-355. (1970)

19. US EPA SW-846. Method for Physical and Chemical Analysis of Solid Waste. Method 6010A. (1972)

20. Pourbaix, M. Atlas of electrochemical equilibria in aqueous solutions. NACE. pp. 257-271; 307-321; 330-342 (1974)

21. Cranston, R.E. and J.W. Murray. The determination of chromium species in natural waters. Analytica Chimica Acta. 99: 276-282. (1978)